



Optimizing bone cement stiffness for vertebroplasty through biomechanical effects analysis based on patient-specific three-dimensional finite element modeling

Yi Peng¹ · Xianping Du² · Lihua Huang³ · Jinsong Li¹ · Ruisen Zhan¹ · Weiguo Wang¹ · Biaoxiang Xu⁴ · Song Wu¹ · Cheng Peng⁵ · Shijie Chen¹ 

Received: 2 January 2018 / Accepted: 9 May 2018 / Published online: 28 May 2018
© International Federation for Medical and Biological Engineering 2018

Abstract

Vertebroplasty is a common and effective treatment for symptomatic osteoporotic vertebral compression fractures. However, the cemented and adjacent vertebrae have a risk of recollapse due to largely unassured mechanisms, among which excessive stiffness of bone cement may be an important risk factor. This study aimed to find the most appropriate range of bone cement stiffness by analyzing its biomechanical effects on the augmented and adjacent vertebrae of individual patient after vertebroplasty. A three-dimensional finite element model of T11-L1 osteoligamentous vertebrae was reconstructed according to individual computed tomography data and validated by post mortem human subject experiment in literatures. Bone cement of varying stiffness was injected into the trabecular core of the T12 vertebrae simultaneously. The maximum von Mises stresses on cancellous and cortical bones of T11-L1 vertebrae were analyzed under the loading conditions of flexion, extension, bending, and torsion. For the adjacent T11 and L1 vertebrae, the stepwise elevation of the bone cement elastic modulus increased the maximum von Mises stress on the cancellous bone, but its effect on cortical bone was negligible. For the augmented T12 vertebra, the stresses on cancellous bone increased slightly under the loading condition of lateral bending and remained no impact on cortical bone. The linear interpolation revealed that the most suitable range of cement elastic modulus is 833.1 and 1408.1 Mpa for this patient. Increased elastic modulus of bone cement may lead to a growing risk of recollapse for the cemented vertebra as well as the adjacent vertebrae. Our study provides a fresh perspective in clinical optimization of individual therapy in vertebroplasty.

✉ Song Wu
songwu08@hotmail.com

✉ Cheng Peng
pcheng83@sina.com

✉ Shijie Chen
shijie_chen_xy3yy@163.com

Yi Peng
pengyi802@hotmail.com

Xianping Du
xianping.du@gmail.com

Lihua Huang
lhhuang2@qq.com

Jinsong Li
50530747@qq.com

Ruisen Zhan
zhrs1960@163.com

Weiguo Wang
xywwg1978@163.com

Biaoxiang Xu
xubiaoxiang@163.com

¹ Department of Orthopaedic Surgery, The Third Xiangya Hospital of Central South University, Changsha 410013, Hunan, China

² Department of Mechanical Engineering, Embry-Riddle Aeronautical University, Daytona Beach, FL 32114, USA

³ Center for Experimental Medicine, The Third Xiangya Hospital of Central South University, Changsha 410013, Hunan, China

⁴ Xiangya Medical School of Central South University, Changsha 410013, Hunan, China

⁵ Department of Burns and Plastic Surgery, The Third Xiangya Hospital of Central South University, Changsha 410013, Hunan, China

Keywords Vertebroplasty · Osteoporotic fracture · Finite element analysis · Bone cement · Elastic modulus

1 Introduction

Osteoporosis (OP), characterized by reducing bone mass and easily fractured bones, is a systemic metabolic disease that occurs in the skeletal parts of the body frequently among the elderly [1, 2]. OP often leads to sudden fracture of a part of the limbs or the vertebral body. The compression fractures of single or multiple vertebral bodies caused by the reduction of bone mineral density and bone strength are named as osteoporotic vertebral compression fractures (OVCFs) [3, 4]. The symptomatic OVCFs frequently result in persistent lumbar back pain in these patients, who are limited in activities of daily life to a large extent and have the potential to cause significant disability and morbidity. Patients with OVCFs can not walk normally, and some patients develop into kyphosis, seriously affecting the quality of their life [5, 6].

Percutaneous vertebroplasty (PVP) and percutaneous kyphoplasty (PKP), the minimally invasive surgery technologies developed in recent years, become the major effective approaches to treat OVCFs. Current practice demonstrates that these technologies produce small trauma, relieve the pain quickly, and restore the height and stability of the fractured vertebral body as much as possible [7–10]. Nevertheless, according to the clinical follow-up observation of the patients after vertebroplasty, the augmented vertebral body and the adjacent vertebral bodies were subjected to fracturing again in some individuals [11–13]. Previous results showed that approximately 50–67% of recurrent fractures occurred at the sites near the enhanced vertebra [14, 15]. Specific mechanisms of recollapse of the vertebrae for individual patients are largely unclear, and studies have shown that the severity of OP, cleft filling pattern of polymethyl methacrylate (PMMA), surgical methods, volume of bone cement, and anti-osteoporosis treatments were all related to the recurrence of the vertebral body fractures [16–18].

PMMA, a synthetic resin commonly used as bone cement in vertebroplasty, not only enhances the height and stability of the vertebral body, but also quickly relieves the pain of patients [19, 20]. PMMA was suspected to be a possible risk factor because of its excessive stiffness [21–23]. Current results regarding the effects of excessive stiffness of PMMA on the stability of augmented vertebra and the adjacent vertebra are inconsistent [24–29]. Therefore, under the circumstances of unifying and standardizing other factors, it is very important to investigate the relationship between bone cement stiffness and refracturing of the vertebral bodies in individual patients. Finding the most suitable ranges of stiffness for bone cement material in clinical can facilitate the pain relief and help rapidly regain quality of life for patients with OVCFs.

To study the effect of bone cement stiffness on the cemented vertebral and adjacent vertebral bodies, a three-dimensional (3D) finite element (FE) model was used. The FE model was considered to be useful in biomechanical studies, and it can avoid the use of human specimens and minimize the variations due to inherent differences among individual parameters [30, 31]. The load-controlled methods consisting gradual elevation of the bone cement elastic modulus were applied to each of the 6 loading conditions: flexion, extension, left/right bending, and left/right torsion. This study was designed to evaluate the changes of the maximum von Mises stresses on both cancellous and cortical bones from the treated and adjacent vertebrae. Our investigation attempts to provide new biomechanical evidence and a fresh perspective into how the vertebroplasty procedure can be implemented more effectively in individuals toward the goal of preventing the recurrence of vertebral compression fractures.

2 Materials and methods

2.1 Overview of the experimental procedures

The outline for specific experimental procedures is shown in Fig. 1. A three-dimensional finite element model of three-level spine segments (T11–L1) was first built. After verifying the validity of the model by previous post mortem human subjects (PMHS) experimental data, the vertebroplasty procedure was simulated by segmenting an irregular cylinder (which functioned as bone cement) on the core of T12 segment. The stiffness (elastic modulus) of this segmented irregular cylinder was changed to simulate the variation of bone cement in batched experiments. The biomechanical effects on the augmented vertebra and the adjacent vertebrae under different conditions were analyzed by measuring the changes of von Mises stresses on the spinal segments. Based on the alterations of vertebral stresses under 6 different loading conditions, the elastic modulus range that balanced the conflict between the recollapse risk and stability of spine segments was determined as the preferred cement stiffness for vertebroplasty.

2.2 Development of T11–L1 thoracolumbar vertebral model

To generate the 3D spinal geometry model comprising T11, T12, and L1, a 75-year-old female patient, with osteoporotic compression fracture in the T12 vertebra which required the treatment of vertebroplasty, was selected. The patient had no other abnormal findings on radiographs. After signing the

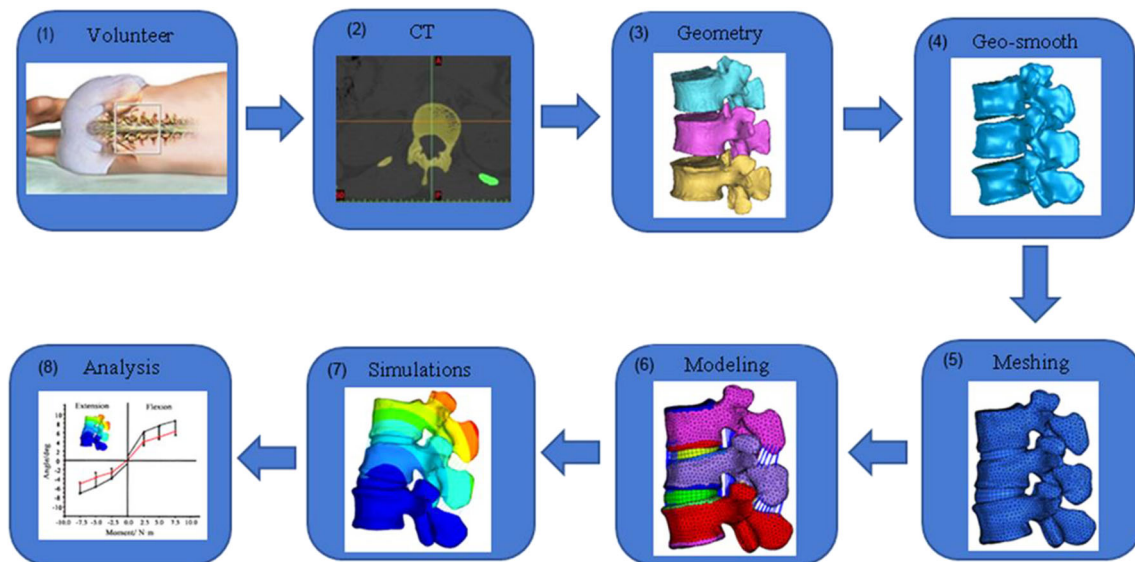


Fig. 1 The research technical route for the biomechanical studies. The stages include the following: (1) volunteer preparation; (2) CT scanning and data collecting; (3) geometry extraction; (4) geometric cleaning; (5)

mesh dividing; (6) material parameter defining; (7) simulation calculating; (8) data analysis and result showing

informed consent, the patient was checked with computed tomographic scans (CT) with 0.2-mm intervals in the thoracolumbar spine segments to get the geometric information. All of the CT images were saved in DICOM format. The image data were imported into the medical 3D reconstruction software Mimics 10.01 (Materialise, Leuven, Belgium). The vertebral geometry model was reconstructed from the scanned images and exported into STL format. To generate a more precise and smooth 3D surface model, the digital geometry model with STL format was imported into the Geomagic Studio12.0 software (Raindrop Geomagic, Inc., Morrisville, NC) for smoothing, polishing, and denoizing (Fig. 2a). The computer-aided design software LS-DYNA 971 (Livermore, CA, USA) was employed to mesh the vertebra, intervertebral disk, and nucleus pulposus. A meshed model of three vertebral segments (T11, T12, and L1) is shown in Fig. 2b. The vertebral body was meshed by tetrahedron to speed the meshing efficiency, while the intervertebral disk is meshed by hexahedron.

One-dimensional beam element was used to simulate the role of ligament, joint capsule, and fascia. Shell elements were used to define vertebral cortical bone, endplate, articular facet joint. “Common node connection” was applied to define the contacts between the articular facet cartilages, cancellous bone, and cortical bone, as well as between endplate and cortical bone. Contact between intervertebral disk and vertebral body, vertebra, and ligaments, as well as between the intervertebral disk and the ligaments, was set with “binding connection”.

The vertebral body was composed of 0.6-mm-thick cortical bone and internal cancellous bone, and the surface was covered with 0.6-mm-thick end plate [32] based on

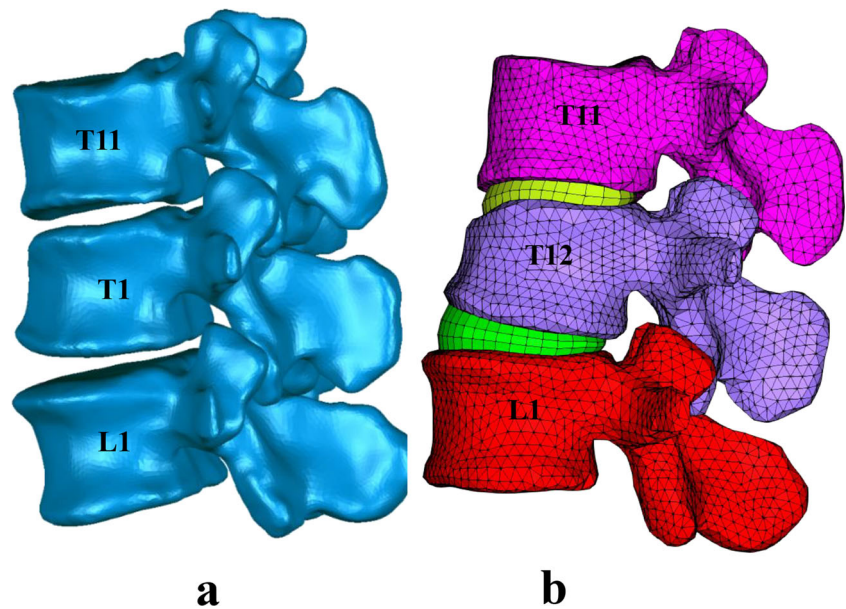
the data in literatures as in Table 1. For the thickness of the vertebral cortical bone, some studies [33–35] measured or calculated as the range 0.1–0.5 mm with average 0.35 mm and used in some studies [36, 37]. However, there are some other studies [38, 39] focused on the measurement of the lower lumbar vertebrae cortical thickness using the PMHS samples and concluded that the average shell thickness of lower vertebrae is around 0.5–0.6 mm. This was used in some modeling processes [40–42] and showed a good result. Furthermore, there are some other studies that use the thickness of 1 mm [43] or 1.5 mm [44] in their finite element models from the CT measurement or some other studies. To balance these aspects, we set the cortical shell thickness as 0.6 mm.

The intervertebral disk consisted of the medullary nucleus and the outer annulus. The nucleus pulposus area was set at 50% of the total area of the intervertebral disk, and the fibrous rings were constructed in a concentric circle at the outer edge of the disk with 10-folds. The whole meshed model of T11-L1 osteoligamentous spine segments is shown in Fig. 3.

2.3 Material properties and element specifications

In this study, the constant loads were used to simulate the daily load. Under these non-heavy daily loads, the bone material can be seen to behave linearly with the change of the load as the simplification. Most of the fractures, except for the accident, are caused by the fatigue and damage accumulation. However, in this study, the loads are in a short term and fatigue can be ignored. Hence, it is enough that most of the components were simulated by the elastic material model, including the spongy bone, cortical bone, interval disk articular facet

Fig. 2 The reconstructed geometric model (a) and the subsequently meshed mode (b) showing the vertebrae and intervertebral disk of three segments (T11, T12, and L1)



cartilage. In addition, the ligaments, as denoted in Fig. 3, were simulated by beam element with the material behavior controlled by some specific force-displacement curves [45].

The material parameters of those mentioned components are shown in Table 1, as referenced from previous reports [46–51]. Furthermore, after the fracture, the material properties of the spine segments, mainly the bone material, would be changed due to the influence of the crack expansion and break of integrity. Considering this effect, the material constants of the model after vertebroplasty were modified based on the previous research [52], as listed in Table 1.

2.4 Meshing size sensitivity study

In the finite element simulation, the meshing size would be important factors for the simulation accuracy. In general, the smaller meshing size could lead to more accurate result, but higher

computational cost and so versus. The most appropriate meshing size always depends on the study problems as demonstrated by the previous researches. In this study, to find the suitable meshing size, the L1 segment was separated from the whole model and used as the base model for meshing sensitivity study, which can save computational time for extra small meshing size model.

As listed in Fig. 4a, the basic loading model, the bottom of L1, was fully constrained and a distributed force was added to the upper surface of this segment. Six meshing sizes, i.e., 0.5, 1, 2.5, 4, 6, and 8 mm, were used in this study as in Fig. 4a. After running 25 ms which is enough for the model to reach load balance, the cancellous bone stress is exported and plotted in Fig. 4b for comparison.

In Fig. 4b, it is obvious that, as the decreasing of the meshing size, the value of cancellous bone stress is increasing. If the meshing size is smaller than 2.5 mm, the stress increases

Table 1 Material properties and element specifications of osteoporotic T11-L1 vertebrae

Anatomical structure	Material structure	Material attribute				Unit type	References
		Density (kg/m ³)	Young's modulus (Mpa)	Poisson's ratio	Thickness (mm)		
Vertebral body	Cortical bone	2000	10,000	0.3	0.6	Shell	[36, 51]
	Fractured cortical bone	2000	8040	0.3	0.6	Shell	[46]
	Cancellous bone	1100	1322	0.19	–	Solid	[36]
	Fractured cancellous bone	1100	449	0.19	–	Solid	[46, 36]
	End plate	2000	670	0.4	0.6	Shell	[32, 46]
Intervertebral disc	Fibrous annulus	1200	5	0.45	–	Solid	[48]
	Nucleus pulposus	1200	9	0.4	–	Solid	[49]
Articular facet cartilage		1360	5.0	0.1	0.5	Shell	[50]

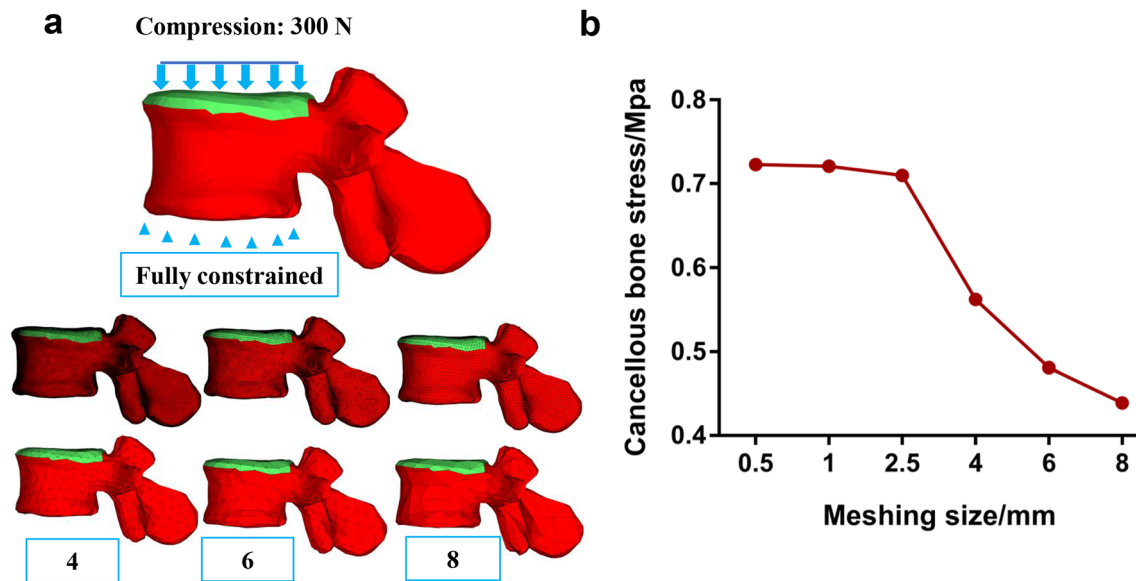


Fig. 3 The whole osteoligamentous model of T11-L1 spine segments

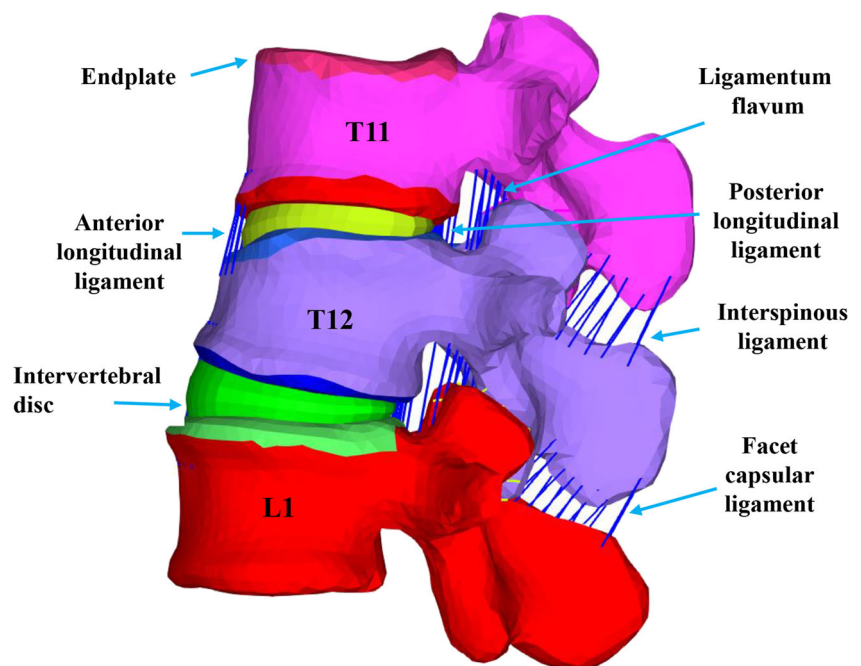
slightly (changing from 2.5 to 1 mm with 1.83% improvement on stress). However, the computational cost increased more than five times as the meshing size from 2.5 mm changed to 1 mm. Considering the computational cost and the computational accuracy, the 2.5 mm meshing size was used in this study.

2.5 Validation of T11-L1 thoracolumbar vertebral model

The validation of the established FE model is critical for the possibility of using model to simulate real responses. Based on the PMHS tests of previous data [53, 54], the developed FE

model using the 75-year-old female data was subjected to 8 loading conditions (flexion, extension, left/right bending, left/right torsion, tension, and compression) to mimic the daily loads of human lumbar spine to validate the biofidelity of the established model, as shown in Fig. 5a. After the validation, the model can be seen as the benchmark model to calculate the suitable cement stiffness by comparing with the model response after vertebroplasty of different stiffness cements. The deformation force was loaded on a rigid shell part generated on the upper surface of spine segment T11. The bottom surface of L1 was fully constrained. For each loading condition, three load levels, as listed in Table 2, were applied to

Fig. 4 Computational accuracy sensitivity study setup with six meshing sizes included (a) and the calculated cancellous bone stress for different meshing size (b)



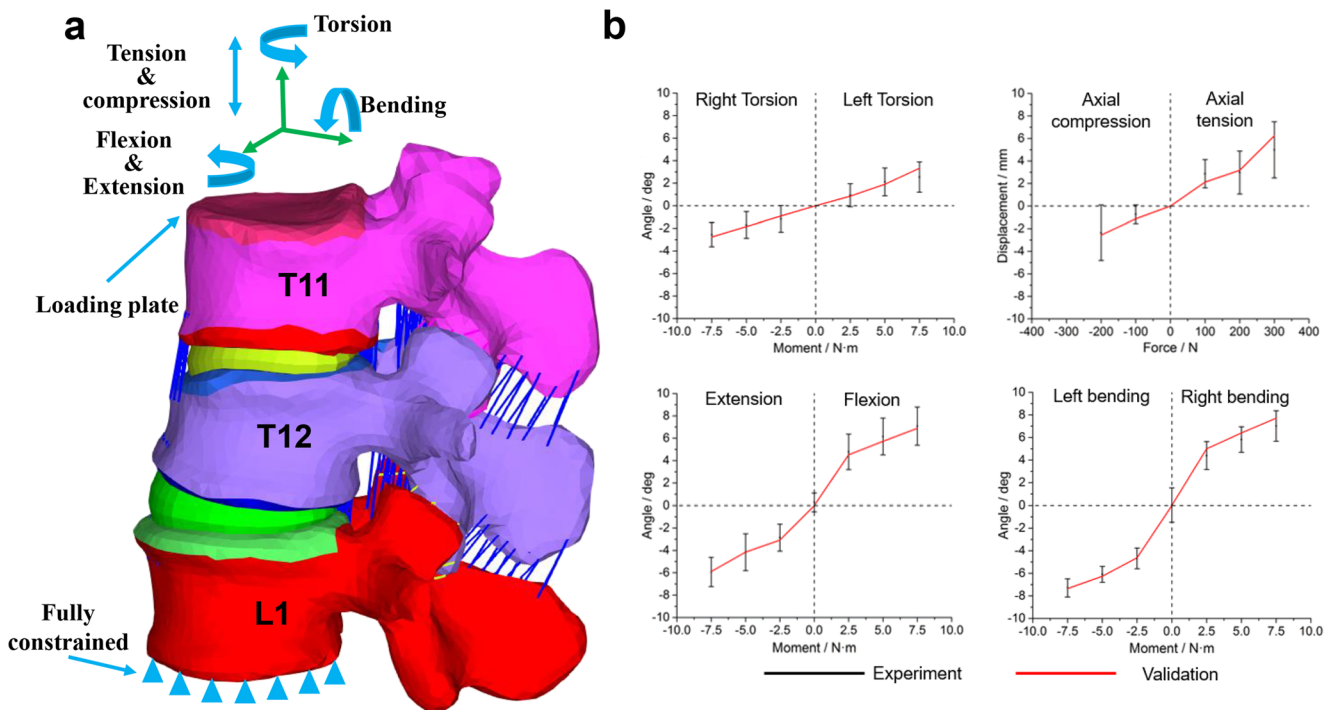


Fig. 5 The validation data of T11-L1 thoracolumbar vertebra. The angle and displacement output of the model (a) under different loading conditions (flexion, extension, left and right lateral bending, and left and right torsion) were obtained. The kinetic data of the model are

within the normal range in the cases of displacement cloud and simulation animation under 8 tested loading conditions and 3 kinds of force levels (b). Each dot indicates the mean value of 3 independent tests. Data shown are mean ± SD from a representative experiment

verify the dynamic responses under different load severity. This further enhanced the computational accuracy and stability of the spine model.

2.6 The modeling of bone cement with different stiffness

The simulation of cement filling was completed based on the knowledge related to clinical treatment of vertebroplasty. The geometry and distribution of the cement filling were defined referring to the X-rays of some treated patients [21]. As previously described [55], bone cement equal to 30% of the volume of the vertebral body was filled to the trabecular core of T12 vertebra. Figure 6 represents a schematic showing the location, shape, and overall size of the bone cement in the vertebral body.

Table 2 Settings of loading conditions for validation of T11-L1 vertebral bodies

Loading conditions	Flexion/extension (N·m)	Lateral bending (N·m)	Torsion (N·m)	Stretching/compression (N)
Level 1	2.5	2.5	2.5	100
Level 2	5	5	5	200
Level 3	7.5	7.5	7.5	300

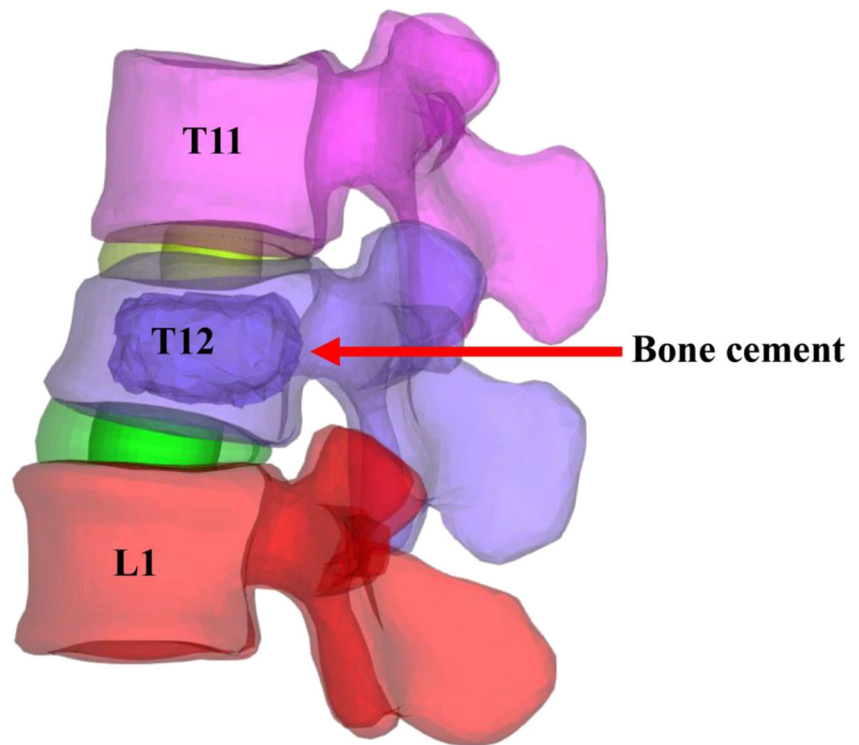
The material properties of the other components were changed based on the fractured parameters in Table 1.

The FE analysis was carried out under six loading cases: flexion/extension, left/right bending, and left/right torsion, with T12 augmented with stiffness-variable bone cement at 18000, 12000, 8000, 4000, 2000, 1000, and 500 MPa. The original FE model, without vertebroplasty, was adopted as the benchmark model to show the differences after the vertebroplasty with different bone cement stiffness. To simulate the weight of human upper body segment, a 500 N axial force was downward loaded on the upper surface of T11 [11, 56]. The bottom of L1 segment was also fully constrained. Furthermore, to validate the biofidelity of the established FE model, some experiments that mimic the regular loads of human spine were adopted, including extension/flexion, left/right bending, and left/right torsion. Based on the setup of experiment [57], the moments of 50, 40, and 30 N·m were loaded on the extension/flexion, left/right bending, and left/right torsion, respectively, as shown in Fig. 5a. The amount and distribution of local Von Mises equivalent stresses on each vertebra were calculated.

2.7 Calculation of suitable elastic modulus range

The linear interpolation method was used to get the appropriate stiffness range reflecting minimum differences between

Fig. 6 The volume of injected bone cement is equivalent to 30% of the volume of T12 vertebral body during in vitro simulation of vertebroplasty



the benchmark model (model without vertebroplasty) and reshaped model (model after vertebroplasty). The points of intersection between the benchmark model stresses and reshaped model stresses of corresponding loading in curves under different cement stiffness were calculated. The intersected value was calculated by using linear interpolation as equation. On a specific interval of stress $[\sigma_0, \sigma_1]$ and elastic moduli $[E_0, E_1]$ for a specific loading condition, the value of the suitable elastic modulus, $E = E_0 + \Delta E \frac{\sigma - \sigma_0}{\sigma_1 - \sigma_0}$, where E is the calculated most suitable bone cement stiffness, σ is the stress value simulated from benchmark model; the σ_0 and σ_1 are two simulated stress values for a specific loading condition and adjacent elastic moduli, which includes the stress value of benchmark model. The E_0 and E_1 are the two adjacent elastic moduli corresponding with σ_0 and σ_1 . ΔE is the length of elastic modulus interval calculated by $\Delta E = E_0 - E_1$. The calculated stiffness values of these intersections were considered as the most suitable under their corresponding loading conditions.

2.8 Statistical analysis

SPSS 19.0 statistical software (Chicago, IL, USA) was used for statistical analysis and data were expressed as mean \pm standard deviation. Comparison between groups was done with ANOVA analysis and χ^2 test. $P < 0.05$ was considered to indicate a statistically significant difference.

3 Results

3.1 Validation of the FE model

Under eight loading conditions (including the flexion, extension, left/right lateral bending, left/right torsion, and stretching and compression), the angle and displacement outputs of the functional spinal units were obtained and compared with previous data obtained from biomechanical experiments of the existing literature [58, 59]. As shown in Fig. 5b, the kinetic data of the model were all within the normal ranges of experiments which showed good response corridors in the cases of displacement cloud and simulation animation under eight tested loading conditions and three kinds of force levels. The fine matching between experiment and simulation suggested that our finite element model of vertebral body had high accuracy and biofidelity, confirming the validity of the present model. This also suggested that our model can be used in the subsequent application of parametric study of bone cement.

3.2 Effects of cement stiffness on augmented T12 vertebra

The dynamic changes of the maximum von Mises stress on the cancellous bone of augmented T12 vertebra in response to cement stiffness alterations are shown in Fig. 7a. With the stepwise increasing of elastic modulus of bone cement from 500 to 18,000 Mpa, the maximum von Mises stress on

cancellous bone of T12 vertebra increased under the loading conditions of lateral bending and decreased slightly under loading cases of flexion and extension (Fig. 7a). The maximum von Mises stress on the cortical bone of T12 vertebra decreased slightly along with the increasing of bone cement elastic modulus under six loading conditions (Fig. 7b) due to the support of cement and fracture weaken of T12 stiffness. Therefore, the loading conditions of lateral bending had obviously more impacts on the T12 maximum von Mises stress compared to the conditions of flexion, extension, and torsion.

3.3 Effects of cement stiffness on adjacent T11 and L1 vertebrae

The impacts of raising elastic modulus of bone cement on both cancellous and cortical bones of the adjacent T11 and L1 vertebrae were also examined. As shown in Fig. 8, in contrast to the cemented T12 vertebra, the maximum Von Mises stress in cancellous bone of T11 and L1 vertebrae increased significantly along with the stepwise raising of bone cement elastic moduli under the loading conditions of flexion and extension (Fig. 8a, c). However, there are no significant changes (all $P > 0.05$) under all other conditions for cancellous bone and cortical bone. The results indicated that the augmentation of T12 vertebra probably increases the risk of compression fractures on the cancellous bones of adjacent vertebrae under flexion and extension working conditions involved in the daily life.

3.4 Calculation of suitable elastic modulus range of bone cement

Our preceding results indicated that the increasing of cement elastic moduli was most likely able to lead to recollapse for the cemented vertebra as well as the adjacent vertebrae (Fig. 7 and

Fig. 8). More specifically, the augmentation of T12 vertebra only impacted six stress responses of the cancellous bone (Fig. 7a), i.e., the flexion and extension of T11 and the left bending and right bending of T12. The changes of the bone cement stiffness almost had no influence on other tests, so they were not considered as subjects used for calculating suitable elastic modulus range in this study. Hence, the FE modeling data from benchmark model and the mentioned six tests were used to estimate the most suitable stiffness range of bone cement. The linear interpolation method was used to compare the values of the intersection points from the datasets generated from our FE model. Decreased bone density in osteoporosis vertebra always results in lower bone material properties and strength [48]. On the other hand, bone cement with high stiffness could cause the high stress concentration on the interface of trabecular bone and cement. As presented in Fig. 9, we selected the range which include the stress of benchmark model for the interpolation and got one interpolated suitable value for each loading condition as in Table 3. Considering six different loading conditions comprehensively, the average and standard error of the suitable cement stiffness (i.e., 1120.6 ± 287.5 Mpa) was considered using these six suitable exact stiffness values. A range rather than a particular value also fits the feasibility of vertebroplasty in clinical, because generally the stiffness of the bone cement cannot be controlled accurately. By this way, the suitable elastic moduli range of bone cement for this specific patient can be determined as 833.1 and 1408 Mpa.

4 Discussion

Percutaneous vertebroplasty is a surgical procedure that has been widely used to treat patients suffering from osteoporotic vertebral compression fractures. However, some patients

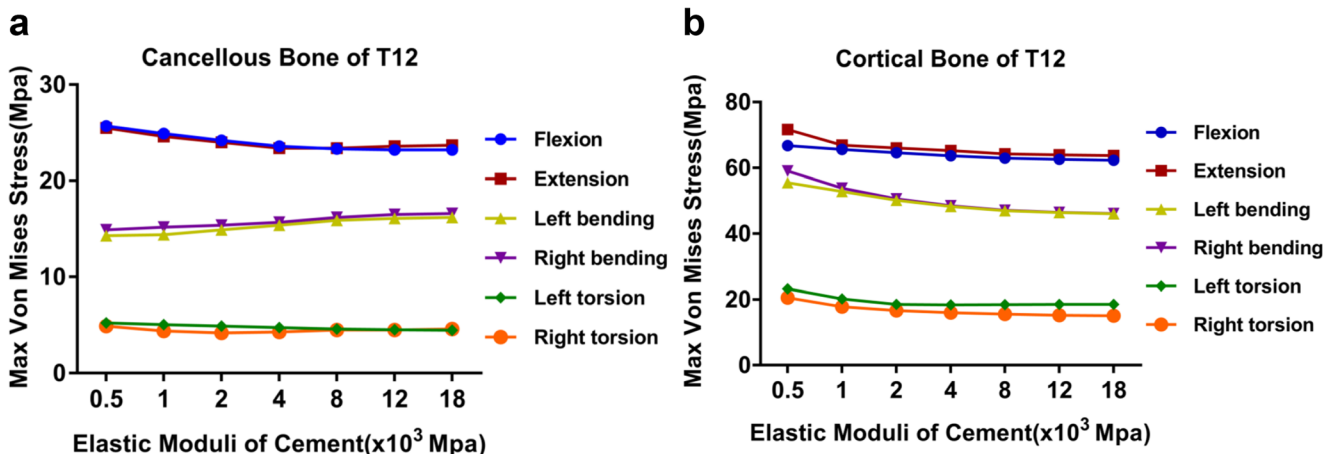


Fig. 7 The changes of maximum von Mises stresses on cancellous bone (a) and cortical bone (b) of cemented T12 vertebra in response to the stepwise elevation of bone cement elastic modulus. Data shown are the results of the von Mises stress changes under the flexion, extension, left/

right bending, and left/right torsion conditions. The bone cement stiffness was increased from 500 to 18,000 MPa, with the cement volume equal to 30% of volume of the T12 vertebra body. Each point indicates the mean value of 3 independent tests

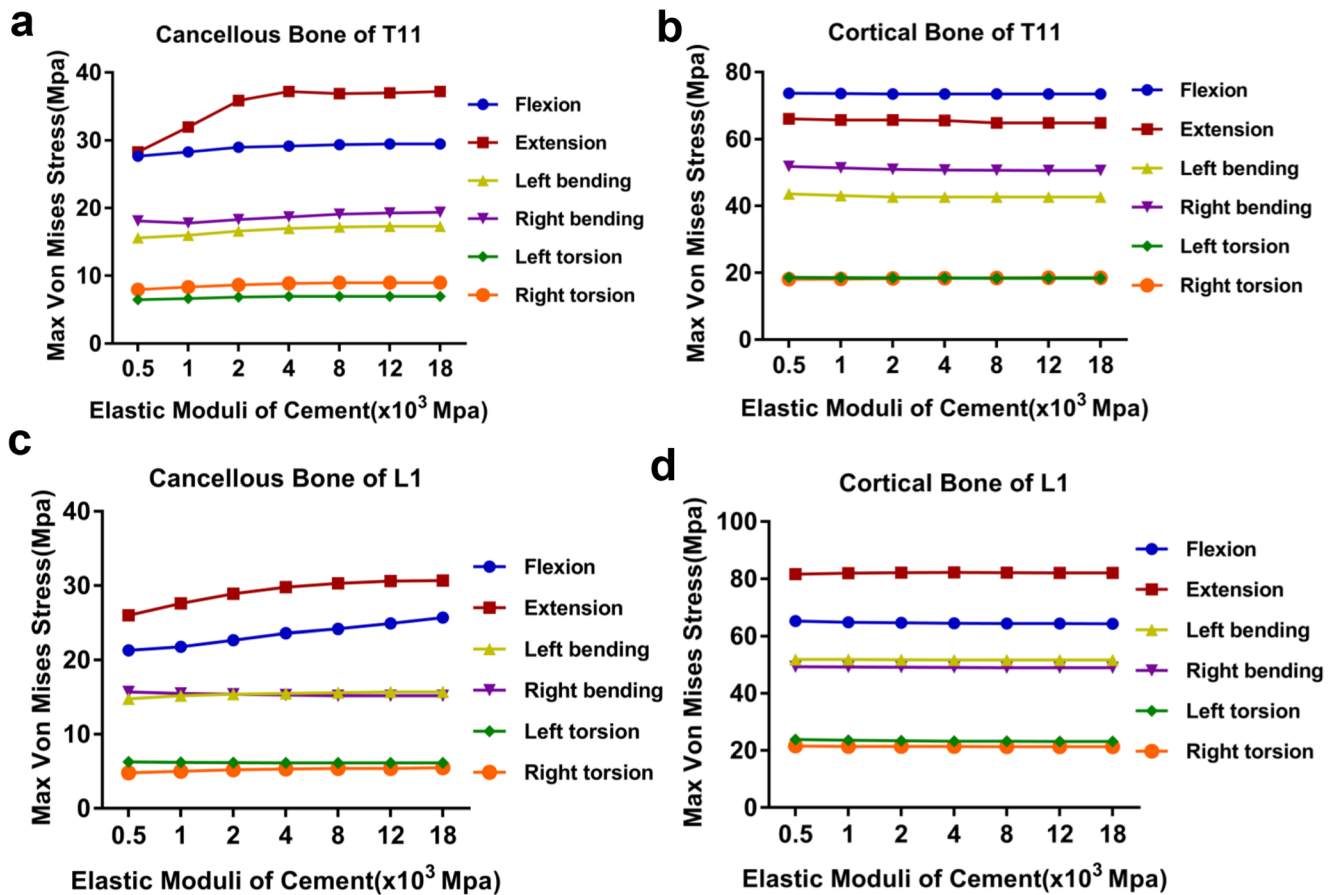


Fig. 8 The changes of maximum von Mises stresses on cancellous bone (a) and cortical bone (b) of adjacent T11 vertebra, and on cancellous bone (c) and cortical bone (d) of adjacent L1 vertebra in response to the stepwise elevation of bone cement elastic modulus. Data shown are the results of the von Mises stress changes under the flexion, extension, left/

right bending, and left/right torsion conditions. The bone cement stiffness was increased from 500 to 18,000 MPa, with the cement volume equal to 30% of volume of the T12 vertebra body. Each point indicates the mean value of 3 independent tests

Fig. 9 Calculation of suitable elastic modulus range by the linear interpolation method

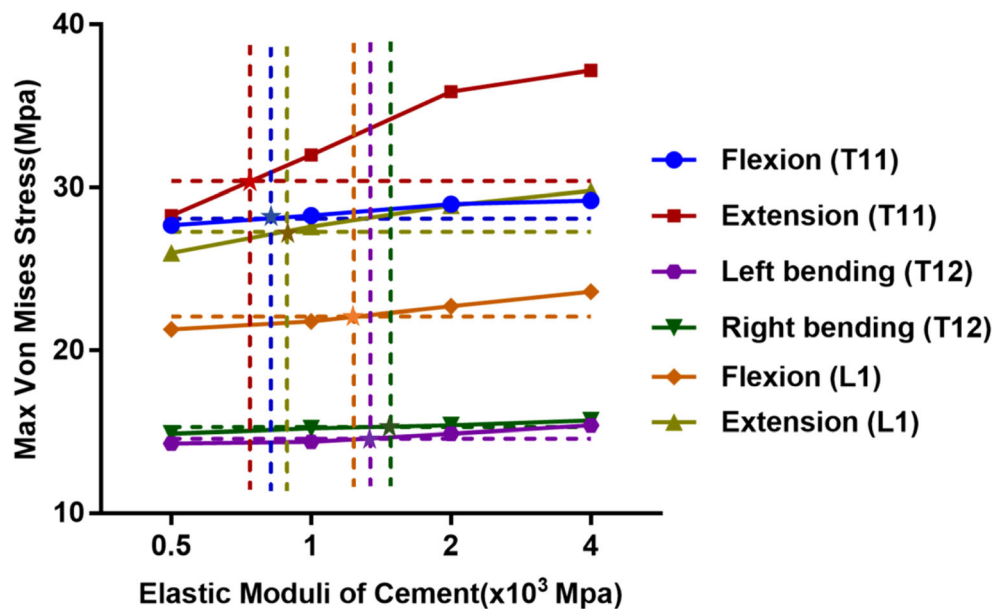


Table 3 Results of optimal stiffness for the 6 loading conditions considering the stress of cancellous bone

Items	Flexion T11	Flexion L1	Extension T11	Extension L1	Left bending T12	Right bending T12
σ_0 (Mpa)	500/27.7 ^a	1000/21.8	500/28.3	500/26.0	1000/14.4	1000/15.2
σ_1 (Mpa)	1000/28.3	2000/22.8	1000/32.0	1000/27.6	2000/14.9	2000/15.4
Benchmark (Mpa)	28.1	22.1	30.4	27.3	14.6	15.3
E (Mpa)	833.3	1300.0	783.8	906.3	1400	1500

^a 500/27.7: means that the stress value under elastic moduli of 500 Mpa is 27.7 Mpa

σ is the stress value simulated from benchmark model; the σ_0 and σ_1 are two simulated stress values for a specific loading condition under adjacent elastic moduli

experience recompression of the PVP-operated vertebrae or new fractures at the neighborhood vertebrae. Using a combined experimental and computational approach, our study suggests that excessive stiffness of bone cement increases the risk of recurrent fractures of the augmented vertebra and the adjacent vertebrae in a 3D finite element model of osteoporotic compression fracture of spine.

Previous reports have suggested that certain parameters of bone cement used in treating vertebral body are potential risk factors for recompression of OVCFs. Accumulating evidence has suggested the critical correlations between modulus of bone cement and the risk of vertebral recollapse in patients after vertebroplasty. In vitro biomechanical study from Boger et al. demonstrates that the failure strength of augmented functional spine units could be better preserved using low-modulus PMMA in comparison to regular PMMA cement [24]. Many studies on 3D finite element analysis showed that excessive stiffness of bone cement can lead to an increased risk of adjacent vertebral fractures following vertebroplasty in osteoporotic FE models [27, 29]. These findings are similar to our results. On the contrary, conclusions of some studies are inconsistent. Pneumaticos et al. revealed that no statistically significant differences of the compressive load of failure could be detected between augmented and non-augmented vertebral bodies [26]. Kim et al. argued that changes on vertebral stress due to the effect of bone cement stiffness alterations can be ignored [25].

Our study found that the maximum von Mises stress on the cancellous bone of cemented vertebra increased gradually with the elevation of the elastic modulus of the injected cement under the loading conditions of lateral bending, which probably due to the extrusion from the adjacent vertebrae to augmented vertebra increased under the loading conditions of lateral bending with the elevation of bone cement stiffness. Besides, the stress of local cancellous bone significantly increased in the active state while stiffness and intensity of bone cement increased [60], which may also lead to fractures of the vertebral body. Therefore, this study also suggests that lowering elastic modulus of bone cement may be a way to reduce postoperative fractures of the vertebral body [48]. The stress in cancellous bone of the adjacent vertebral bodies under different loading cases increased significantly along with the changes in the

elastic modulus of bone cement, which mainly because that the stress in cancellous bone of adjacent vertebrae can be elevated by increasing vertebral rigidity through filling bone cement, which increases contact stiffness on some local areas on the adjacent vertebrae and raises the likelihood of fracture. Therefore, the clinical injection of excessive stiffness bone cement should not be pursued, and this helps with minimizing the risks of bone cement leakage and potential secondary fractures.

Our results based on the model derived from personalized fracture patterns are more clinically relevant than other model using just non-fracture FSUs [24], and this approach on determining mechanical parameters definitely facilitates the better understanding of how to achieve improvement in the human application. The FE modeling technique has the advantage over in vitro experimental methods that a number of different treatment scenarios can be examined using the same initial model. However, most of these FE modeling studies investigate vertebroplasty simulated using generic architecture models with idealized cement shapes or oversimplified material modeling. The vertebral morphology and bone material properties are confirmed to play significant roles in the mechanical response of the vertebra under axial load [61, 62]. Recently, it is reported that the effectiveness of percutaneous vertebroplasty is determined by the patient-specific bone condition and the treatment strategy, since the effectiveness was strongly influenced by interactions between local bone qualities, cement volume, and injection location [63]. Thus, there is an urgent need to develop specimen-specific spinal models both to verify the model predictions more robustly and to assess the effect of vertebroplasty across the whole patient cohort [64]. One of the main objects of our work was to establish the level of accuracy for the subject-specific FE models of individual vertebrae with and without cement augmentation. Our report here represents our effects on a first step toward the development and verification of such models using a combined experimental and computational approach. Our results together with other reports [28, 65–67] convincingly demonstrate that FE modeling with integrated computerized tomography is a useful tool for personalized predicting in situ vertebral fracture load resulting from vertebroplasty.

The finite element model has several limitations in the study and interpretation of clinical phenomena and mechanisms. One limitation is that our finite model was built from one person's data that cannot represent all patients treated with vertebroplasty. Furthermore, we used a simplified finite element model that did not refine the type of vertebral compression fractures. The clinical practice of vertebroplasty rather than the in vitro simulation of our model may change the shape of the vertebral body, so the results of this study still need confirmation by clinical long-term follow-up data. Besides, the 3D FE model used in the study did not attach the paravertebral muscle tissue, and the muscles generally stabilized the spine during normal thoracolumbar movement. In addition, the material parameters of this study model were based on the existing literature, and there were no material parameter settings for the bone mineral density and CT data, which can represent the uniqueness of the sample. Further studies are needed to collect the results of FE analyses based on quantitative values such as CT grayscale, bone mineral density [65]. In addition, these bone material inhomogeneity properties due to the density differ of porous and micro-structures would have influence on the stress distribution and transmission on the scale of bone trabecula [36]. In this study, the result focuses on the stress changes before and after vertebroplasty with different cement stiffness. As a qualitative study, the bone material was homogenized. For future study, if the stress on bone trabecula level, e.g., to observe the interaction effect between the bone trabecula stress and damage and the cement stiffness, the inhomogeneity should be considered. It is no doubts that the general experiences based on datasets of multiple individuals will assist the development of bone cement with most appropriate stiffness to better treat individual patients by vertebroplasty.

5 Conclusions

Our results suggest that lowering the elastic modulus of bone cement can reduce the augmented and adjacent vertebral body stress as well as the occurrence of fractures. Since there is no mature experience on low elastic modulus cement in clinical, our study provides a theoretical basis and a feasible approach for determining the suitable stiffness range of bone cement. Our research sheds further light on optimizing the stiffness of bone cement to develop better personalized strategies for conducting vertebroplasty.

Acknowledgments Finite element analyses were performed at the Department of Mechanical Engineering, Embry-Riddle Aeronautical University. The authors specially thank Xianping Du for technical assistance. This study was funded by the grants of the New Xiangya Talent Project of the Third Xiangya Hospital of Central South University (JY201502).

Authors' contribution Shijie Chen and Yi Peng designed the study and wrote the first draft of the manuscript. Jinsong Li, Biaoxiang Xu, and Weiguo Wang collected the data. Xianping Du completed finite element

modeling, computation and analysis. Cheng Peng, Song Wu, Lihua Huang, and Ruisen Zhan participated in data analysis and interpretation and revision of the manuscript. All authors have approved the final version of the paper.

Funding This study was funded by the grants of the New Xiangya Talent Project of the Third Xiangya Hospital of Central South University (JY201502).

Compliance with ethical standards

Conflict of interest The authors declare that they have no conflict of interest.

Research involving human participants and/or animals Not applicable.

Informed consent Not applicable.

References

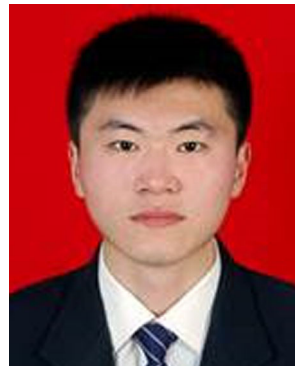
- Rosen CJ, Ingelfinger JR (2016) Building better bones with biologics - a new approach to osteoporosis? *N Engl J Med* 375(16):1583–1584
- An J, Yang H, Zhang Q, Liu C, Zhao J, Zhang L, Chen B (2016) Natural products for treatment of osteoporosis: the effects and mechanisms on promoting osteoblast-mediated bone formation. *Life Sci* 147:46–58
- Parreira P et al (2017) An overview of clinical guidelines for the management of vertebral compression fracture: a systematic review. *Spine J* 17:1932–1938
- Zhao S, Xu CY, Zhu AR, Ye L, Lv LL, Chen L, Huang Q, Niu F (2017) Comparison of the efficacy and safety of 3 treatments for patients with osteoporotic vertebral compression fractures: a network meta-analysis. *Medicine (Baltimore)* 96(26):e7328
- Garg B, Dixit V, Batra S, Malhotra R, Sharan A (2017) Non-surgical management of acute osteoporotic vertebral compression fracture: a review. *J Clin Orthop Trauma* 8(2):131–138
- Svensson HK, Olsson LE, Hansson T, Karlsson J, Hansson-Olofsson E (2017) The effects of person-centered or other supportive interventions in older women with osteoporotic vertebral compression fractures—a systematic review of the literature. *Osteoporos Int* 28:2521–2540
- Mehbod, A., S. Aunoble, and J.C. Le Huec, Vertebroplasty for osteoporotic spine fracture: prevention and treatment. *Eur Spine J*, 2003 12 Suppl 2: p. S155–62
- Clark W, Bird P, Diamond T, Gonski P (2015) Vertebroplasty for acute painful osteoporotic fractures (VAPOUR): study protocol for a randomized controlled trial. *Trials* 16:159
- Rosenbaum BP, Kshetry VR, Kelly ML, Mroz TE, Weil RJ (2017) Trends in inpatient Vertebroplasty and Kyphoplasty volume in the United States, 2005–2011: assessing the impact of randomized controlled trials. *Clin Spine Surg* 30(3):E276–E282
- Kan SL, Yuan ZF, Chen LX, Sun JC, Ning GZ, Feng SQ (2017) Which is best for osteoporotic vertebral compression fractures: balloon kyphoplasty, percutaneous vertebroplasty or non-surgical treatment? A study protocol for a Bayesian network meta-analysis. *BMJ Open* 7(1):e012937
- Chen LH, Hsieh MK, Liao JC, Lai PL, Niu CC, Fu TS, Tsai TT, Chen WJ (2011) Repeated percutaneous vertebroplasty for refracture of cemented vertebrae. *Arch Orthop Trauma Surg* 131(7):927–933
- Uppin AA, Hirsch JA, Centenera LV, Pfeifer BA, Pazianos AG, Choi IS (2003) Occurrence of new vertebral body fracture after percutaneous vertebroplasty in patients with osteoporosis. *Radiology* 226(1):119–124
- Zhang L, Wang Q, Wang L, Shen J, Zhang Q, Sun C (2017) Bone cement distribution in the vertebral body affects chances of

- recompression after percutaneous vertebroplasty treatment in elderly patients with osteoporotic vertebral compression fractures. *Clin Interv Aging* 12:431–436
14. Aquarius R, Homminga J, Verdonshot N, Tanck E (2011) The fracture risk of adjacent vertebrae is increased by the changed loading direction after a wedge fracture. *Spine (Phila Pa 1976)* 36(6):E408–E412
 15. Voormolen MH et al (2006) Prospective clinical follow-up after percutaneous vertebroplasty in patients with painful osteoporotic vertebral compression fractures. *J Vasc Interv Radiol* 17(8):1313–1320
 16. Lin WC, Lee YC, Lee CH, Kuo YL, Cheng YF, Lui CC, Cheng TT (2008) Refractures in cemented vertebrae after percutaneous vertebroplasty: a retrospective analysis. *Eur Spine J* 17(4):592–599
 17. Ha KY, Kim YH (2013) Risk factors affecting progressive collapse of acute osteoporotic spinal fractures. *Osteoporos Int* 24(4):1207–1213
 18. Rho YJ, Choe WJ, Chun YI (2012) Risk factors predicting the new symptomatic vertebral compression fractures after percutaneous vertebroplasty or kyphoplasty. *Eur Spine J* 21(5):905–911
 19. He Z, Zhai Q, Hu M, Cao C, Wang J, Yang H, Li B (2015) Bone cements for percutaneous vertebroplasty and balloon kyphoplasty: current status and future developments. *J Orthopaedic Translation* 3(1):1–11
 20. Bae H, Hatten HP Jr, Linovitz R, Tahernia AD, Schaufele MK, McCollom V, Gilula L, Maurer P, Benyamin R, Mathis JM, Persenaire M (2012) A prospective randomized FDA-IDE trial comparing Cortoss with PMMA for vertebroplasty: a comparative effectiveness research study with 24-month follow-up. *Spine (Phila Pa 1976)* 37(7):544–550
 21. Heini PF, Walchli B, Berlemann U (2000) Percutaneous transpedicular vertebroplasty with PMMA: operative technique and early results. *A prospective study for the treatment of osteoporotic compression fractures*. *Eur Spine J* 9(5):445–450
 22. Tai, C.L., et al., Modification of Mechanical Properties, Polymerization Temperature, and Handling Time of Polymethylmethacrylate Cement for Enhancing Applicability in Vertebroplasty. *Biomed Res Int*, 2016. **2016**: p. 7901562
 23. Hoppe S, Wangler S, Aghayev E, Gantenbein B, Boger A, Benneker LM (2016) Reduction of cement leakage by sequential PMMA application in a vertebroplasty model. *Eur Spine J* 25(11):3450–3455
 24. Boger A, Heini P, Windolf M, Schneider E (2007) Adjacent vertebral failure after vertebroplasty: a biomechanical study of low-modulus PMMA cement. *Eur Spine J* 16(12):2118–2125
 25. Kim JM, Shin DA, Byun DH, Kim HS, Kim S, Kim HI (2012) Effect of bone cement volume and stiffness on occurrences of adjacent vertebral fractures after vertebroplasty. *J Korean Neurosurg Soc* 52(5):435–440
 26. Pneumaticos SG, Triantafyllopoulos GK, Evangelopoulos DS, Hipp JA, Heggeness MH (2013) Effect of vertebroplasty on the compressive strength of vertebral bodies. *Spine J* 13(12):1921–1927
 27. Cho AR, Cho SB, Lee JH, Kim KH (2015) Effect of augmentation material stiffness on adjacent vertebrae after osteoporotic Vertebroplasty using finite element analysis with different loading methods. *Pain Physician* 18(6):E1101–E1110
 28. Wijayathunga VN, Oakland RJ, Jones AC, Hall RM, Wilcox RK (2013) Vertebroplasty: patient and treatment variations studied through parametric computational models. *Clin Biomech (Bristol, Avon)* 28(8):860–865
 29. Takano H, Yonezawa I, Todo M, Mazlan MH, Sato T, Kaneko K (2016) Biomechanical study of the effects of balloon Kyphoplasty on the adjacent vertebrae. *J Biomedical Sci Engineering* 9(10):478–487
 30. Winking M, Stahl JP, Oertel M, Schnettler R, Böker DK (2004) Treatment of pain from osteoporotic vertebral collapse by percutaneous PMMA vertebroplasty. *Acta Neurochir* 146(5):469–476
 31. Kosmopoulos V, Keller TS (2004) Damage-based finite-element vertebroplasty simulations. *Eur Spine J* 13(7):617–625
 32. Kurutz, M. and L. Oroszváry, Finite Element Modeling and Simulation of Healthy and Degenerated Human Lumbar Spine. 2012: INTECH Open Access Publisher
 33. Silva MJ, Wang C, Keaveny TM, Hayes WC (1994) Direct and computed tomography thickness measurements of the human, lumbar vertebral shell and endplate. *Bone* 15(4):409–414
 34. Whitehouse WJ, Dyson ED, Jackson CK (1971) The scanning electron microscope in studies of trabecular bone from a human vertebral body. *J Anat* 108(Pt 3):481–496
 35. Ritzel H, Amling M, Pösl M, Hahn M, Dellling G (1997) The thickness of human vertebral cortical bone and its changes in aging and osteoporosis: a histomorphometric analysis of the complete spinal column from thirty-seven autopsy specimens. *J Bone Miner Res* 12(1):89–95
 36. Blanchard, R., Morin C., Malandrino A., Vella A., Sant Z., Hellmich C., Patient-specific fracture risk assessment of vertebrae: a multiscale approach coupling X-ray physics and continuum micromechanics. *Int J Numer Method Biomed Eng*, 2016. 32(9): e02760. <https://doi.org/10.1002/cnm.2760>
 37. Malandrino A, Noailly J, Lacroix D (2013) Regional annulus fibre orientations used as a tool for the calibration of lumbar intervertebral disc finite element models. *Comput Methods Biomech Biomed Engin* 16(9):923–928
 38. Fazzalari NL, Parkinson IH, Fogg QA, Sutton-Smith P (2006) Antero-postero differences in cortical thickness and cortical porosity of T12 to L5 vertebral bodies. *Joint Bone Spine* 73(3):293–297
 39. Roberts S, McCall IW, Menage J, Haddaway MJ, Eisenstein SM (1997) Does the thickness of the vertebral subchondral bone reflect the composition of the intervertebral disc? *Eur Spine J* 6(6):385–389
 40. Oxland TR (2016) Fundamental biomechanics of the spine—what we have learned in the past 25 years and future directions. *J Biomech* 49(6):817–832
 41. Ellingson AM, Shaw MN, Giambini H, An KN (2016) Comparative role of disc degeneration and ligament failure on functional mechanics of the lumbar spine. *Comput Methods Biomech Biomed Engin* 19(9):1009–1018
 42. Wagnac E, Arnoux PJ, Garo A, Aubin CE (2012) Finite element analysis of the influence of loading rate on a model of the full lumbar spine under dynamic loading conditions. *Med Biol Eng Comput* 50(9):903–915
 43. Baroud G, Nemes J, Ferguson SJ, Steffen T (2003) Material changes in osteoporotic human cancellous bone following infiltration with acrylic bone cement for a vertebral cement augmentation. *Comput Methods Biomech Biomed Engin* 6(2):133–139
 44. Lu YM, Hutton WC, Gharpuray VM (1996) Can variations in intervertebral disc height affect the mechanical function of the disc? *Spine (Phila Pa 1976)* 21(19):2208–2216 discussion 2217
 45. Ren, H., Shen Y., Zhang Y.Z., Ding W.Y., Xu J.X., Yang D.L., Cao J.M., Correlative factor analysis on the complications resulting from cement leakage after percutaneous kyphoplasty in the treatment of osteoporotic vertebral compression fracture. *J Spinal Disord Tech*, 2010. 23(7): p. e9–15
 46. Polikeit A, Nolte LP, Ferguson SJ (2003) The effect of cement augmentation on the load transfer in an osteoporotic functional spinal unit: finite-element analysis. *Spine (Phila Pa 1976)* 28(10):991–996
 47. Silva MJ, Keaveny TM, Hayes WC (1997) Load sharing between the shell and centrum in the lumbar vertebral body. *Spine (Phila Pa 1976)* 22(2):140–150
 48. Kurutz M, Oroszvary L (2010) Finite element analysis of weightbath hydrotraction treatment of degenerated lumbar spine segments in elastic phase. *J Biomech* 43(3):433–441
 49. Chen SH, Tai CL, Lin CY, Hsieh PH, Chen WP (2008) Biomechanical comparison of a new stand-alone anterior lumbar interbody fusion cage with established fixation techniques - a three-dimensional finite element analysis. *BMC Musculoskelet Disord* 9:88

50. Galbusera F, Schmidt H, Wilke HJ (2012) Lumbar interbody fusion: a parametric investigation of a novel cage design with and without posterior instrumentation. *Eur Spine J* 21(3):455–462
51. Rohlmann A, Zander T, Schmidt H, Wilke HJ, Bergmann G (2006) Analysis of the influence of disc degeneration on the mechanical behaviour of a lumbar motion segment using the finite element method. *J Biomech* 39(13):2484–2490
52. Han KS, Rohlmann A, Yang SJ, Kim BS, Lim TH (2011) Spinal muscles can create compressive follower loads in the lumbar spine in a neutral standing posture. *Med Eng Phys* 33(4):472–478
53. Panjabi MM, Krag MH, White AA 3rd, Southwick WO (1977) Effects of preload on load displacement curves of the lumbar spine. *Orthop Clin North Am* 8(1):181–192
54. Panjabi MM, Oxland TR, Yamamoto I, Crisco JJ (1994) Mechanical behavior of the human lumbar and lumbosacral spine as shown by three-dimensional load-displacement curves. *J Bone Joint Surg Am* 76(3):413–424
55. Belkoff SM, Mathis JM, Erbe EM, Fenton DC (2000) Biomechanical evaluation of a new bone cement for use in vertebroplasty. *Spine (Phila Pa 1976)* 25(9):1061–1064
56. Lo YP, Chen WJ, Chen LH, Lai PL (2008) New vertebral fracture after vertebroplasty. *J Trauma* 65(6):1439–1445
57. Kim YJ, Lee JW, Park KW, Yeom JS, Jeong HS, Park JM, Kang HS (2009) Pulmonary cement embolism after percutaneous vertebroplasty in osteoporotic vertebral compression fractures: incidence, characteristics, and risk factors. *Radiology* 251(1):250–259
58. Qiu TX, Teo EC, Zhang QH (2006) Effect of bilateral facetectomy of thoracolumbar spine T11-L1 on spinal stability. *Med Biol Eng Comput* 44(5):363–370
59. Xu G, Fu X, du C, Ma J, Li Z, Ma X (2014) Biomechanical effects of vertebroplasty on thoracolumbar burst fracture with transpedicular fixation: a finite element model analysis. *Orthop Traumatol Surg Res* 100(4):379–383
60. Zhang L et al The biomechanical effects of osteoporosis vertebral augmentation with cancellous bone granules or bone cement on treated and adjacent non-treated vertebral bodies: A finite element evaluation. *Clinical Biomechanics* 25(2):166–172
61. Jones AC, Wilcox RK (2007) Assessment of factors influencing finite element vertebral model predictions. *J Biomech Eng* 129(6):898–903
62. Wilcox RK (2007) The influence of material property and morphological parameters on specimen-specific finite element models of porcine vertebral bodies. *J Biomech* 40(3):669–673
63. Widmer Soyka RP, Helgason B, Hazrati Marangalou J, van den Bergh JP, Rietbergen B, Ferguson SJ (2016) The effectiveness of percutaneous Vertebroplasty is determined by the patient-specific bone condition and the treatment strategy. *PLoS One* 11(4):e0151680
64. Wijayathunga VN, Jones AC, Oakland RJ, Furtado NR, Hall RM, Wilcox RK (2008) Development of specimen-specific finite element models of human vertebrae for the analysis of vertebroplasty. *Proc Inst Mech Eng H* 222(2):221–228
65. Matsuura Y, Giambini H, Ogawa Y, Fang Z, Thoreson AR, Yaszemski MJ, Lu L, An KN (2014) Specimen-specific nonlinear finite element modeling to predict vertebrae fracture loads after vertebroplasty. *Spine (Phila Pa 1976)* 39(22):E1291–E1296
66. Chent, X., H. Li, and X. Yang. A Patient-Specific Approach to Assessment of Biomechanical Stability Following Percutaneous Vertebroplasty Using CT Images. In 2007 IEEE/ICME International Conference on Complex Medical Engineering 2007
67. Tarsuslugil SM, O'Hara RM, Dunne NJ, Buchanan FJ, Orr JF, Barton DC, Wilcox RK (2014) Experimental and computational approach investigating burst fracture augmentation using PMMA and calcium phosphate cements. *Ann Biomed Eng* 42(4):751–762



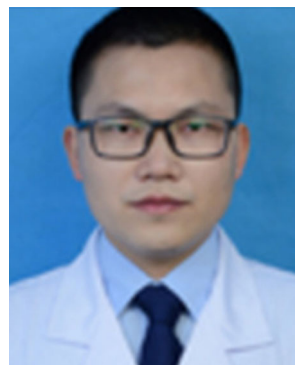
Yi Peng, Ph.D. candidate, Department of Orthopedic Surgery, The Third Xiangya Hospital of Central South University, Changsha, Hunan 410013, China



Xianping Du, Ph.D. candidate, Department of Mechanical Engineering, Embry-Riddle Aeronautical University, Daytona Beach, FL 32114, USA



Lihua Huang, Ph.D. Center for Experimental Medicine, The Third Xiangya Hospital of Central South University, Changsha, Hunan 410013, China



Jinsong Li, M.D., Ph.D., Department of Orthopedic Surgery, The Third Xiangya Hospital of Central South University, Changsha, Hunan 410013, China



Ruiseng Zhan , M.D., Ph.D.
Department of Orthopedic Surgery,
The Third Xiangya Hospital of
Central South University,
Changsha, Hunan 410013, China



Song Wu , M.D., Ph.D.
Department of Orthopedic Surgery,
The Third Xiangya Hospital of
Central South University,
Changsha, Hunan 410013, China



Weiguo Wang , M.D. Department
of Orthopedic Surgery, The Third
Xiangya Hospital of Central South
University, Changsha, Hunan
410013, China



Cheng Peng , M.D., Ph.D.
Department of Burns and Plastic
Surgery, The Third Xiangya
Hospital of Central South
University, Changsha, Hunan
410013, China



Biaoxiang Xu , undergraduate,
Xiangya Medical School of
Central South University,
Changsha, Hunan 410013, China



Shijie Chen , M.D., Ph.D.,
Department of Orthopedic
Surgery, The Third Xiangya
Hospital of Central South
University, Changsha, Hunan
410013, China